

Numerical Simulation Support for Diffusion Coefficient Measurements in Polycrystalline Thin Films

Alain Portavoce^{1,a,*}, Ivan Blum^{1,b}, Lee Chow^{2,c}, Jean Bernardini^{1,d},
Dominique Mangelinck^{1,e}

¹CNRS, IM2NP, Faculté des Sciences de Saint-Jérôme, case 142, 13397 Marseille, France

²Department of Physics, University of Central Florida, Orlando, Florida 32816, USA

^aalain.portavoce@im2np.fr, ^bivan.blum@im2np.fr, ^cchow@mail.ucf.edu, ^djean.bernardini@im2np.fr,
^edominique.mangelinck@im2np.fr

Keywords: Diffusion, Poly-Crystals, Measurements, Finite Elements Simulation, Fisher Geometry.

Abstract. The measurement of diffusion coefficients in today's materials is complicated by the down scaling of the studied structures (nanometric effects in thin films, nano-crystalline layers, etc.) and by the complex production process conditions of industrial samples or structures (temperature variations, complex solute and point defect distributions, stress gradients, etc.). Often diffusion measurements have to be performed in samples for which initial experimental conditions do not offer the possibility of using conventional diffusion analytical solutions. Furthermore, phenomena involved with diffusion are sometimes so numerous and complex (stress, matrix composition inhomogeneities, time dependence of point defect generation sources, electrical effects, clustering effects, etc...) that the use of analytical solutions to solve the observed diffusion behavior is difficult. However, simulations can be of use in these cases. They are time consuming compared to the use of analytical solutions, but are more flexible regarding initial conditions and problem complexity. The use of simulations in order to model physical phenomena is quite common nowadays, and highly complex models have been developed. However, two types of simulations have to be considered: i) simulations aiming to understand and predict phenomena, and ii) simulations for measurement purposes, aiming to extract the (average) value of a physical parameter from experimental data. These two cases have different constraints. In the second case, that is the subject of this article, one of the most important stress is that the simulation has to precisely scale the experiment (sample size, experiment duration, etc.), sometimes preventing the measurement due to computational time consumption. Furthermore, the simpler the model (small number of parameters) used in the simulation, the more relevant the measurement (minimum error). In this paper, examples of recent works using two- and three-dimensional finite element simulations for diffusion coefficient measurements in thin polycrystalline films and nano-crystalline layers are presented. The possible use of simulations for diffusion coefficient measurements considering GB migration, GB segregation, or triple junctions is also discussed.

Introduction

Atomic diffusion in solids is an important phenomenon as it controls kinetics of material evolutions towards several types of equilibrium states (phase formation, bulk composition, surface and interface segregation...). It takes place in many industrial processes related to structural and functional material production, especially in metallurgy and microelectronic fabrication processes. The measurement of diffusion coefficients allows to understand and to predict atom transport in solids. Often, diffusion coefficients are extracted from experimental one-dimensional (1D) composition profiles measured after controlled (temperature- T -, time- t - and atmosphere) thermal treatments, using analytical solutions [1] or numerical simulations [2] of the diffusion process, taking into account the sample geometry and experimental conditions. Analytical diffusion solutions have the benefit to procure exact results in a minimum of time. However, they are restricted to given

initial conditions and given boundary conditions, and they are usually obtained for reduced complexity diffusion problems. Their use is mainly limited by experimental conditions that may not match available analytical models. Numerical simulations are time consuming and include numerical errors. They are principally limited by computer performances (speed and memory size). However, they can be used for highly complex problems (several interrelated physical models), for a wide kind of sample geometry (1D, 2D and 3D) and experimental conditions, and if the model is carefully designed (physics laws, geometry, boundary conditions, discretization), the numerical error can be kept at a negligible level. Because industrial process conditions are often far from equilibrium, numerical simulations are extensively used in industry. They allow a significant gain of time and an important decrease of production costs. For example, the cost reduction of microelectronic device production associated to modeling and simulation was evaluated to be up to 40% by the International Technology Roadmap for Semiconductors ITRS in 2007 [3]. Because of industrial needs, powerful commercial softwares designed for finite element simulations (FES) of a wide range of engineering and scientific problems are available (Flux-Expert, Sentaurus, Ansys, Comsol and others). A lot of companies have simulation teams that use these softwares in the research, development and production fields. It is important to note that to be used for industry applications, simulations have to fulfill several requirements: i) they should reproduce experimental condition variations during the process (stress, temperature, atmosphere...), ii) at the experimental scale (size –m, cm, μm , nm, and time –seconds, minutes, hours), iii) the results must be quantitative, iv) they should be obtained in a minimum time scale, and v) the simulations' support (software) should be as friendly as possible to use, allowing frequent modifications performed by different users. Impurity diffusion coefficient measurements, as well as diffusion simulations in mono-crystalline Si (mono-Si) are widely performed in one- and two-dimensions using FES [4]. However, despite intensive FES of mass transport and of grain boundary motion in poly-crystals [5-10], diffusion coefficients in poly-crystals are mainly measured in strict kinetic regime conditions (A, B or C) using analytical solutions (Fisher's model for the regime B, for example) [1]. Recently, Gryaznov et al. (2008) [11] have used FES (software Flux-Expert) with a modified-Fisher geometry to study impurity diffusion in poly-crystalline ionic compounds. They performed two-dimensional simulations and converted the 2D results in 1D profiles in order to compare the effects of the model geometry upon experimental profiles, but no diffusion coefficients were measured. Fournier Dit Chabert et al. (2007) [12] have performed 1D FES of surface and grain boundary (GB) segregation using the software Comsol Multiphysics. Their results were in good agreement with the McLean analytical model. Using their simulations to fit Auger electron spectroscopy measurements, they were able to measure the diffusion coefficient of S in a Ni-based(001) superalloy, and thus, were able to predict S segregation in the Ni superalloy GBs versus grain size.

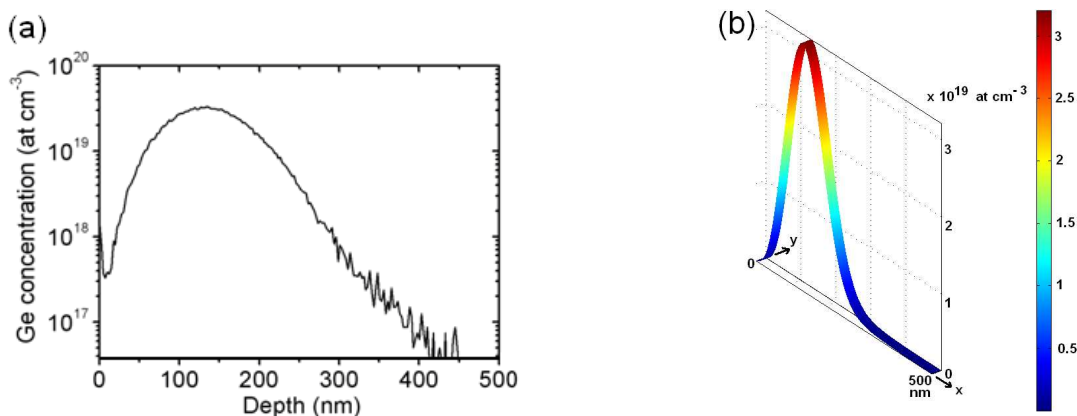


Figure 1. 1D experimental SIMS profile before annealing (a), and the corresponding 2D initial distribution defined in the 2D model (b).

Finite element simulations and 2D Fisher's geometry

Benefits. Few years ago (2007) [13], we showed that FES can be used to measure simultaneously diffusion coefficients in poly-crystalline thin films' grains and GBs, for experiments in the kinetic regime *B*, using the 2D Fisher geometry. This is a significant benefit compared to the usual procedure using analytical type *B* regime solutions that consist in measuring the GB diffusion coefficient (D_{gb}) in poly-crystals once the grain (lattice) diffusion coefficient (D_g) has been measured in mono-crystalline samples [1]. Actually, it should be noted that 2D FES do not need to know the exact kinetic regime during experiments, and can simulate diffusion between the usually considered regimes [14]. The FES-based method consists in using the initial 1D experimental profile to define the initial atom distribution in the 2D geometry, and once the 2D calculations has been performed (annealing simulations), to convert the final 2D distribution in an 1D profile, and to compare it with the experimental final profile. Fig. 1 presents the Ge profile measured by secondary ion mass spectrometry (SIMS) in a 500 nm-thick polycrystalline Si (poly-Si) layer before annealing, and its corresponding 2D Ge distribution in the 2D geometry made of half of a grain (20 nm) and half of a GB (0.25 nm) along the *y* axis (Fisher-type geometry [15]). The impurity distribution before annealing is considered to be identical in the grain and in the GB. Fig. 2 shows the simulation results (2D and 1D) corresponding to a thermal treatment at 900 °C for 0.5 hour, and its comparison with the experimental SIMS profile.

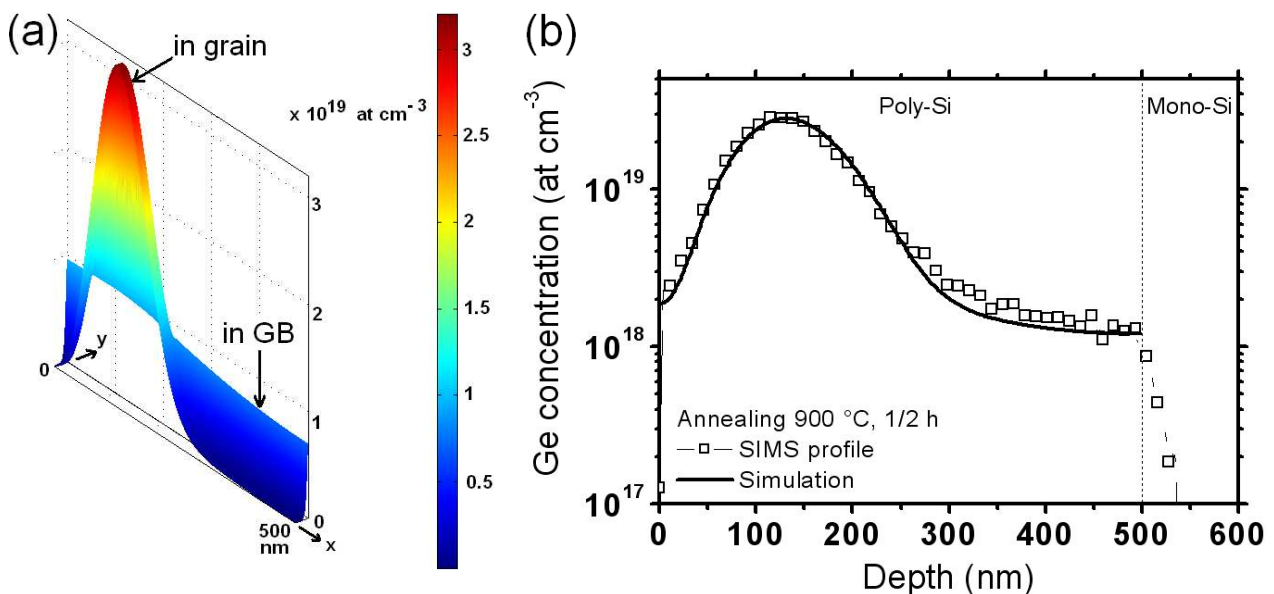


Figure 2. 2D simulation results (a), and the corresponding 1D distribution profile compared to the experimental SIMS profile measured after annealing at 900 °C for 0.5 hour (b).

Consistent with the Fisher model [15], D_g and D_{gb} were considered to be constant during annealing (*Fickian* diffusion [1,16]). After each simulation, the 2D distribution is averaged along the *x* axis (layer thickness) in order to obtain a 1D profile similar to the profiles measured experimentally (fig. 2). Depending on the agreement between simulated and experimental 1D profiles, D_g and D_{gb} are changed in order to get the best fit between simulations and experiments. Because D_g and D_{gb} have different effects on the 1D profile [13], only one set of these coefficients corresponds to a single profile, with an error generally between 5 and 20%. This error varies with the difference in total dose of atoms between the profiles measured before and after annealing, due to the intrinsic inaccuracies of the methods used to measure the profiles [17]. The measurement error of the coefficients D_g and D_{gb} can be defined independently, considering the several D_g - D_{gb} pairs corresponding to fits that are not the best, but that are still acceptable considering the inaccuracy of profile measurements.

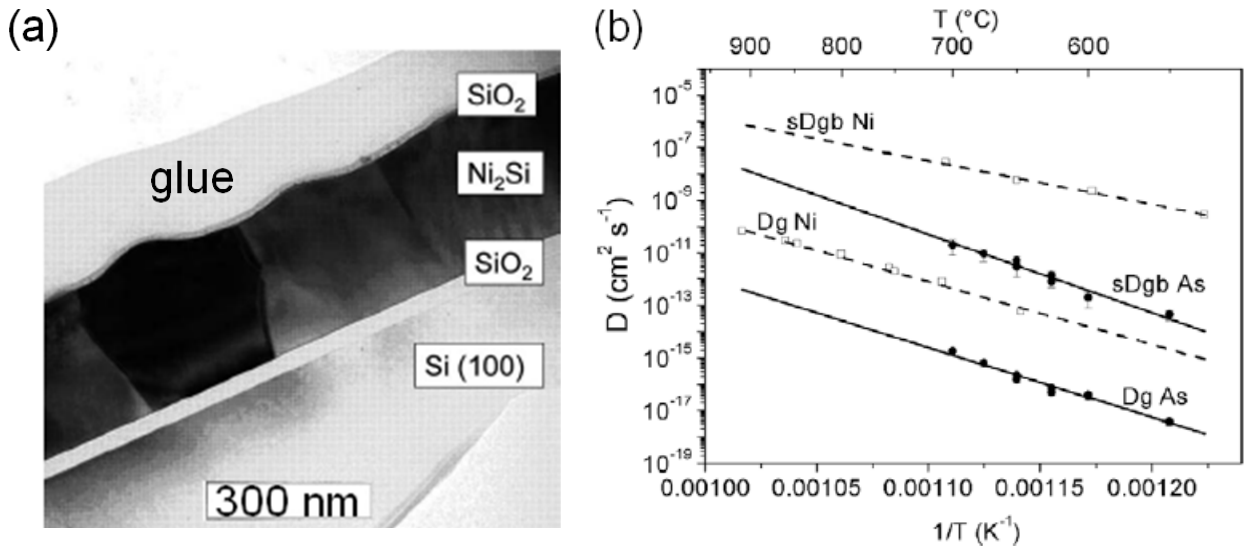


Figure 3. TEM cross-section image of a Ni₂Si layer implanted with As atoms (a), and As lattice and GB diffusivities measured in this layer using 2D FES [18-19], compared to Ni diffusion in Ni₂Si [29] (b).

One of the FES benefits is to be able to use different models than Fisher's model, which may not have analytical solutions (not resolved yet or not possible to resolve analytically). As an illustration, we present in fig. 3 the As diffusivity measured using FES in a Ni₂Si thin film exhibiting columnar grains [18-19]. The Ni₂Si layer was encapsulated between two SiO₂ thin layers (20–30 nm) preventing As desorption from the surface, and As diffusion in the substrate. The Ni₂Si layer was implanted with a 5×10^{15} at cm⁻² dose of As ions at 120 keV. Fig. 3a presents transmission electron microscopy (TEM) measurements performed on the layer, and fig. 3b shows D_g and sD_{gb} we measured, s being the segregation coefficient of As in the Ni₂Si GBs that we could not separate from the GB diffusion coefficient. It can be noted that the method described here allows to measure lattice diffusion coefficients at low temperatures (fig. 3b, $T \leq 700$ °C), as the composition profile in the kinetic regime *B* is sensitive to very small diffusion lengths in the grains (few nanometers), which are usually not possible to measure in mono-crystalline samples via the same experimental techniques (SIMS...) [20-21].

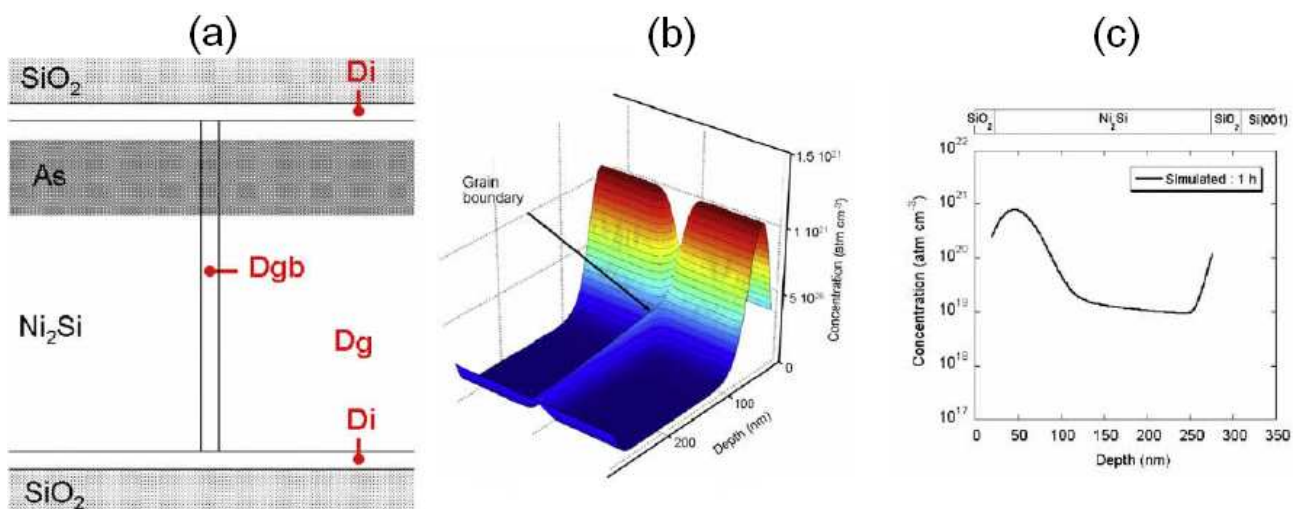


Figure 4. 2D model (a), 2D simulation results (b), and 1D simulation results (c) [19].

For these measurements, we used the flexibility of FES to define a slightly modified Fisher's model that takes into account atomic diffusion at the two SiO₂/Ni₂Si interfaces (fig. 4). GB and interface segregation were not considered in the model. As shown in fig. 4a, three diffusion coefficients were defined: i) D_g related to lattice diffusion in grains, ii) D_{gb} the GB diffusivity, and iii) D_i

corresponding to the diffusivity at the SiO₂ /Ni₂Si interfaces [18-19]. Figs. 4b and 4c show an example of simulated As distribution obtained after annealing for 1 hour with $D_g = 1.5 \times 10^{-16}$, $D_{gb} = 3.8 \times 10^{-12}$ and $D_i = 1 \times 10^{-4} \text{ cm}^2 \text{ s}^{-1}$ (interface diffusion considered to be infinitely fast [18]). Even without interface segregation, interface boundaries can act as diffusion sources for grains, as shown in figs. 4b and 4c (end of the 1D profile). The possibility offered by FES to measure in-grain lattice diffusion in poly-crystalline layers is of great interest. For example, one application is the measurement of the average lattice diffusion coefficient in nano-crystalline materials. Diffusion in nano-grains has been poorly studied due to experimental issues. However, FES using the Fisher geometry allows to measure the lattice diffusion in nanometers-wide grains and to compare this diffusivity with lattice diffusion in mono-crystals. Fig. 5 presents the in-grain Ge lattice diffusion and the Ge GB diffusion measured in a 500 nm-thick poly-Si layer made of 40 nm-wide grains [22]. The Ge nano-lattice diffusion D_g is compared to Ge bulk diffusion D_b in mono-Si [23-25] in fig. 5a, and the nano-GB diffusion coefficient nano- D_{gb} is compared to the micro-GB diffusion coefficient micro- D_{gb} measured in poly-Si made of 30 μm -wide grains [22].

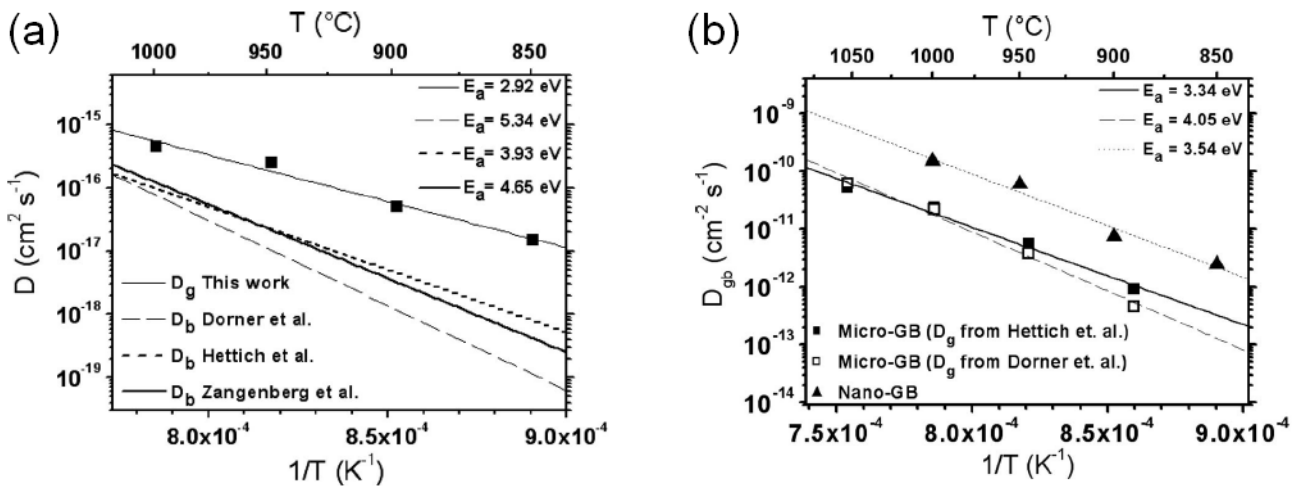


Figure 5. (a) Ge lattice diffusion in 40 nm-wide Si grains (solid squares) compared to Ge lattice diffusion in mono-Si [23-25], and (b) Ge diffusion in nano-GBs (solid triangles) compared to Ge diffusion in micro-GBs [22].

Ge lattice diffusion was found to be one order of magnitude faster in 40 nm-wide Si grains than in mono-Si, with an activation energy in the nano-grains about 1 eV smaller than in mono-Si. Ge diffusion in nano-GB was found to be one order of magnitude faster than in micro-GB, however, similar activation energies were found in the two types of GBs.

Grain boundary segregation. FES allow to solve diffusion problems in poly-crystals considering GB segregation. Fig. 6 presents FES results obtained using the Fisher geometry and considering McLean's GB segregation. In this case, three parameters can be measured at given temperature: D_g and D_{gb} , as well as s the segregation coefficient. However, the effects of D_{gb} and s on the diffusion profile cannot be separated, meaning that these two parameters cannot be extracted simultaneously from a single profile. For example, if D_{gb} is measured from diffusion experiments performed in the kinetic regime C [14], D_g and s can be simultaneously measured from a single diffusion profile using FES. Fig 6a presents simulated 1D profiles obtained with $t = 360 \text{ s}$, $D_g = 5 \times 10^{-17}$, $D_{gb} = 5 \times 10^{-13} \text{ cm}^2 \text{ s}^{-1}$, and $s = 1, 10$ or 1000 . Fig. 6b presents the fit of the results presented in fig. 6a using the analytical solution of the problem in the case of a semi-infinite poly-crystal, which allows to measure the triple product $sD_{gb}\delta$ if D_g is known ($\delta = 0.5 \text{ nm}$ being the lateral size of the GB), thanks to the equation $sD_{gb}\delta = 1.308 \times (D_g/t)^{1/2} \times (-\partial \ln C / \partial x^{6/5})^{-5/3}$ [1]. Without segregation ($s = 1$) the GB diffusion coefficient extracted from the analytical solution is quite close to the real value, as we found $D_{gb} = 4.05 \times 10^{-13}$ instead of $5 \times 10^{-13} \text{ cm}^2 \text{ s}^{-1}$. However, important errors upon either s or

D_{gb} are made if $s > 1$, which are principally due to the influence of atom reflection at the interface (thin film) that is not taken into account in the analytical model (semi-infinite film) [1].

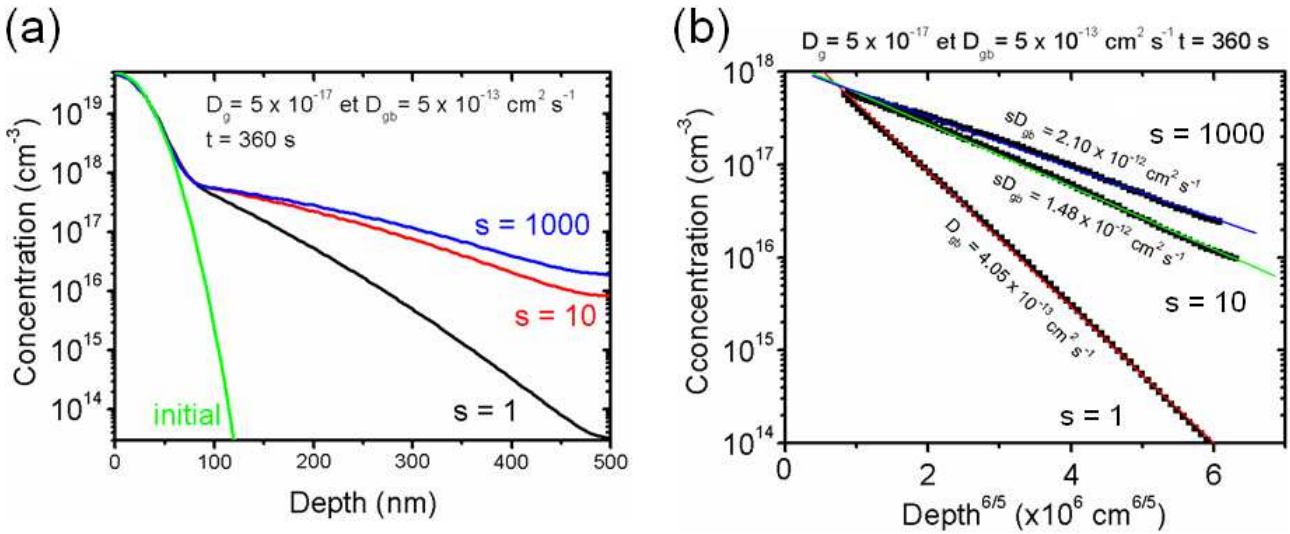


Figure 6. Results of 2D FES of impurity diffusion in a poly-crystal using the Fisher geometry (40 nm grains) with $D_g = 5 \times 10^{-17}$ and $D_{gb} = 5 \times 10^{-13} \text{ cm}^2 \text{ s}^{-1}$, and considering that the GB segregation coefficient $s = 1, 10$ or 1000 . The diffusion time was $t = 360 \text{ s}$. (a) 1D diffusion profiles, and (b) fit of the simulated profiles with an analytical solution for semi-infinite poly-crystalline layers.

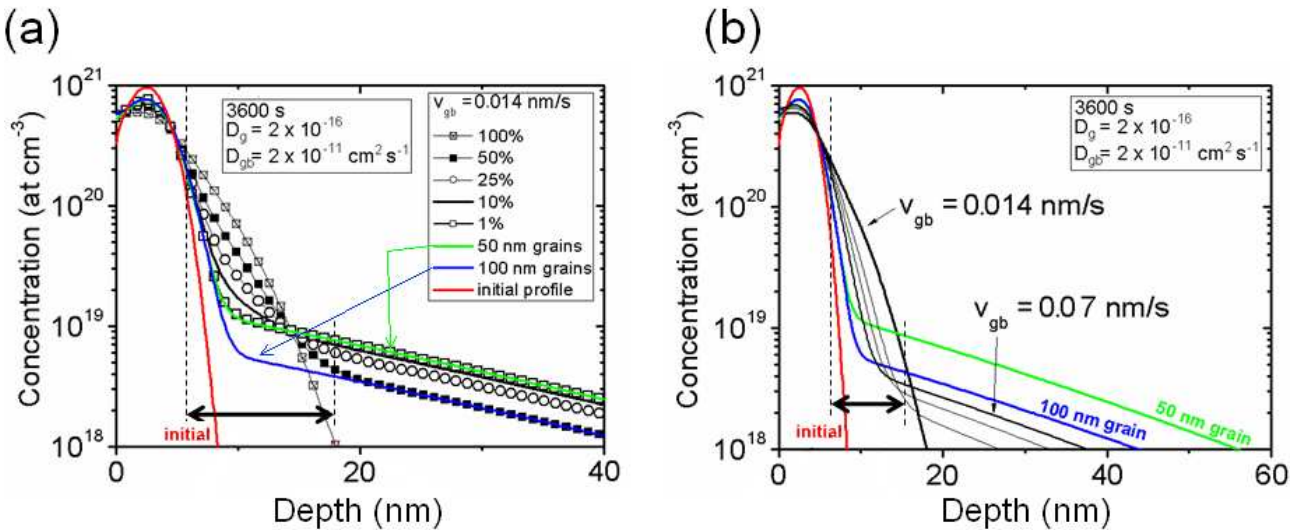


Figure 7. 1D profiles obtained from 2D FES using the Fisher geometry with growing grain (from 50 nm to 100 nm) and moving GB, with $D_g = 2 \times 10^{-16}$, $D_{gb} = 5 \times 10^{-11} \text{ cm}^2 \text{ s}^{-1}$, and $t = 3600 \text{ s}$: (a) for different fraction of growing grains and $v_{gb} = 0.014 \text{ nm s}^{-1}$, and (b) for different grain growth rates if all the grains are growing.

Moving grain boundaries. During annealing of poly-crystals, grains can grow and thus GBs can move. We usually do our best to perform diffusion experiments in conditions avoiding grain growth. However, diffusivities are often extracted from reactive diffusion experiments (oxide and silicide growth [26] for example) in order to understand phases' growth and to predict their kinetics during fabrication processes. It is thus interesting, in some cases, to study atomic transport in GBs during grain growth, and to measure an effective diffusion coefficient. A simple model can use the Fisher model [15] including a lateral movement of the GB, as well as an increasing grain size versus time. Similar to the case of GB segregation, the model possesses three constant parameters: D_g and D_{gb} , as well as v_{gb} the GB displacement rate (or grain growth rate). If we consider that not all the

grains are growing, the fraction of growing grains f_{gr} can be a fourth parameter. Of course, all these parameters cannot be measured simultaneously on a single diffusion profile.

However, v_{gb} can be measured using in situ X-ray diffraction for example [27], D_g can be measured individually as usual [20-21], and both introduced into the model. Thus, an effective D_{gb} related to grain growth can be extracted from experiments. Fig. 7 presents 1D profiles calculated from 2D FES with $D_g = 2 \times 10^{-16}$, $D_{gb} = 5 \times 10^{-11} \text{ cm}^2 \text{ s}^{-1}$, and $t = 3600 \text{ s}$, in the case of 50 nm-wide grains growing up to a lateral size of 100 nm (the double of their initial size). The profiles related to diffusion in similar conditions but with grains of constant size of either 50 or 100 nm are also presented in fig. 7. If $v_{gb} = 0.014 \text{ nm s}^{-1}$, the grains grow during the entire annealing time. If all the grains are growing, the diffusion profile resembles to a profile corresponding to diffusion through a single phase [1], and could be misinterpreted as resulting from pure lattice diffusion, or diffusion in the kinetic regimes *A* or *C* [14]. Fig. 7a shows the variations of the diffusion profile versus the fraction of growing grains if $v_{gb} = 0.014 \text{ nm s}^{-1}$. If 1% of the grains are growing ($f_{gr} = 0.01$), the diffusion profile is superimposed to the profile corresponding to the non-growing 50 nm-wide grains. The effect of grain growth is not detectable on the diffusion profile. However, if 10% of the grains are growing ($f_{gr} = 0.1$), the grain growth effect on the profile is not negligible anymore. The modification may mislead the experimentalist that can interpret the first part of the profile, including the grain-growth related change, as resulting from lattice diffusion in grains, leading to the overestimation of D_g . One can note that in our simulations, the maximum depth of the first part of the profile is less than 20 nm, which is smaller than the critical length $5 \times \sqrt{(D_g t)}$ ($= 42 \text{ nm}$ in our case) usually considered in analytical solutions as the maximum depth on experimental profiles that can reach atoms diffusing in grains. Deeper in the sample, the slopes of all the profiles are identical to the slope of the profiles of 50 and 100 nm-wide non-growing grains (except if $f_{gr} = 1$), indicating that the same diffusion coefficient can be extracted from the profile slopes using an analytical solution of the Fisher model [1]. Fig. 7b presents the variations of the diffusion profile in function of the grain growth rate v_{gb} . If the grains are not growing during the entire annealing time ($v_{gb} > 0.014 \text{ nm s}^{-1}$), the profile looks like to result from diffusion through a poly-crystal in the kinetic regime *B*. However, it is not superimposed to either the profiles of 50 or 100 nm-wide non-growing grains. Similar to the case of growing grains, it exhibits a modified zone having a depth less than 20 nm. If v_{gb} is fast, the grains reach a lateral size of 100 nm faster, and the deep part of the profile tends to get superimposed to the profile related to diffusion in a poly-crystal of constant 100 nm-wide grains.

Finite element simulations and 3D geometry

Description. Similar to 2D FES, simulations using a three-dimensional (3D) geometry can be used to simulate 1D diffusion experiments in poly-crystals. In order to minimize the calculation time, the symmetries of the 3D geometry is used to define the smaller volume that can be used to solve the diffusion problem. Fig. 8a presents the geometry used to simulate diffusion in a 500 nm-thick poly-crystalline layer made of 40 nm-wide grains having a square shape (3D Fisher's geometry). This volume contained 1/8 of the total 3D Fisher's geometry. In the same way as for the 2D geometry, the experimental 1D profile measured before annealing is used to define the 3D initial profile in the 3D geometry (fig 8a), and after the simulation, the 3D distribution is transformed in a 1D profile that can be compared to experimental composition profiles (fig. 8b). If the Fisher geometry is used in 3D, D_g and D_{gb} are the only parameters, and they can be measured simultaneously on single profiles using the same procedure as previously described for 2D models.

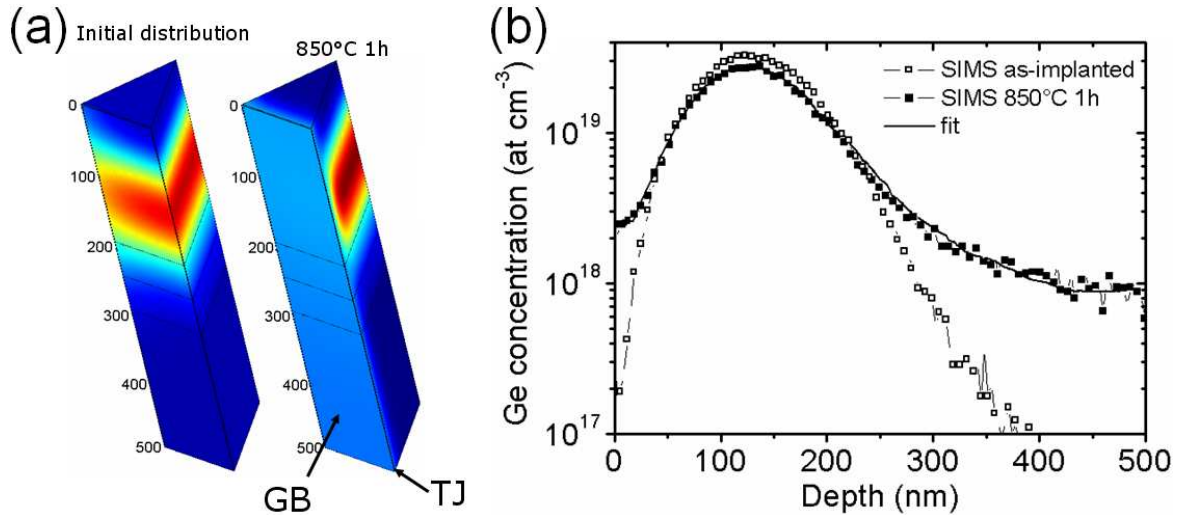


Figure 8. 3D geometry used to simulate diffusion via FES in a poly-crystalline thin film having square-shaped 40 nm-wide grains (a), and the resulting 1D diffusion profile compared to the experimental profile after annealing at 850°C for 1 hour (b).

Triple junctions. The use of a 3D geometry can be of high interest in order to measure diffusion coefficients in triple junctions (TJs). In the 3D geometry presented in fig. 8a, both GB and TJ diffusion paths are taken into account in addition to in-grain lattice diffusion using the Fisher geometry. In this geometry, the GB corresponds to a 0.5 nm-thick plane and the TJ corresponds to a square pipe having a section of 0.25 nm². Using this geometry, we can analyze the same Ge diffusion profiles (figs. 1 and 2) measured in a 500 nm-thick nano-crystalline Si layer made of 40 nm-wide grains, which we previously studied using the 2D Fisher geometry via FES (fig. 5). Fig. 9a presents the SIMS profile measured after the diffusion of Ge at 850°C for 1 hour in the nano-crystalline Si layer, with simulated profiles obtained using the 3D FES with D_g equal to the coefficient measured in the nano-grains using 2D FES (2D- D_g), and D_{gb} equal to the coefficient measured in poly-Si having micrometric grains (micro- D_{gb}) in same conditions, and with the TJ diffusion coefficient D_{tj} having a value between 1×10^{-11} and 1×10^{-9} cm² s⁻¹, corresponding to a ratio D_{tj}/D_{gb} from 5×10^1 to 5×10^3 in agreement with the literature [28].

The influence of TJ diffusion in the Si nano-crystalline layer is not negligible as the final 1D profile is highly dependent upon the value of D_{tj} . Furthermore, the SIMS profile is correctly reproduced by the simulations if a GB diffusion similar to the one measured in micro-crystalline Si is used with $D_{tj} \sim 1 \times 10^{-10}$ cm² s⁻¹. If D_{tj} is maintained constant ($= 1 \times 10^{-9}$ cm² s⁻¹ for example), 3D FES can be used to extract D_g and D_{gb} as previously done using the 2D geometry. In this case, the 3D- D_g is found identical to the 2D- D_g , while the 3D- D_{gb} is found smaller than the 2D- D_{gb} and close to the micro- D_{gb} [28]. In nano-crystalline Si, the diffusivity in GB is the same as in micro-crystalline Si. The faster diffusion of Ge in nano-Si is due to a diffusion increase in nano-grains (lower vacancy formation energy) and fast diffusion in TJs [28]. Fig 9b presents the coefficients of diffusion measured in TJs considering that GB diffusion in nano-crystalline Si is identical with GB diffusion in micro-crystalline Si. We found $D_{tj} = 5.72 \times 10^4 \exp(-3.24 \text{ eV} / kT)$ cm² s⁻¹ with $D_{tj}/D_{gb} \sim 4.7 \times 10^2$ [28].

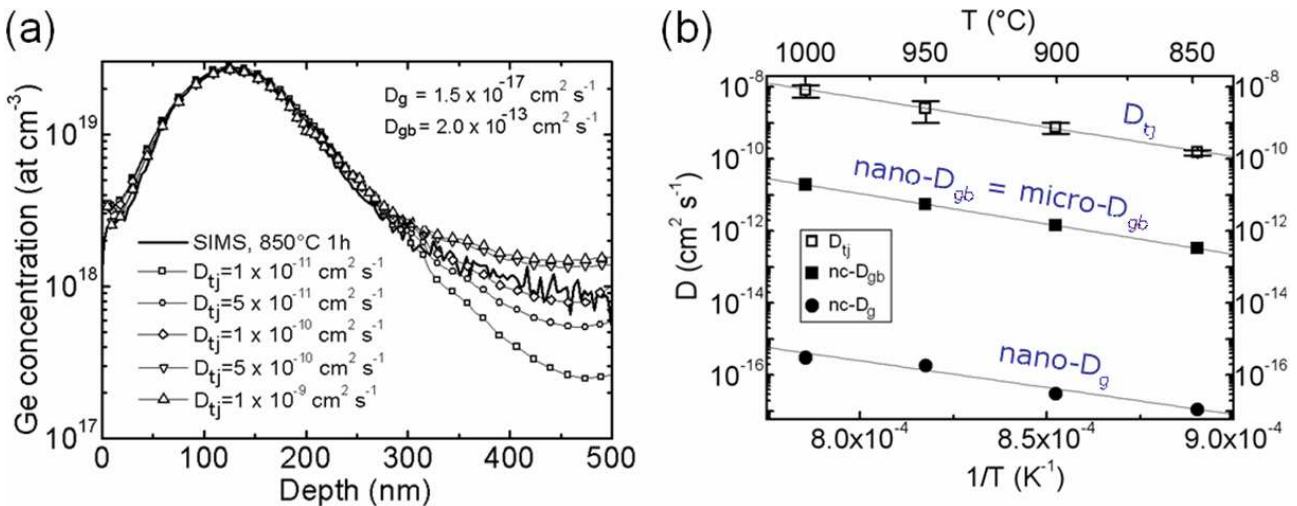


Figure 9. Ge SIMS profile measured in nano-crystalline Si after annealing at 850°C for 1 hour (solid line) compared to simulated profiles using 3D FES with $D_g = 1.5 \times 10^{-17}$, $D_{gb} = 2 \times 10^{-13}$ and $1 \times 10^{-11} \leq D_{tj} \leq 1 \times 10^{-9}$ cm² s⁻¹ (a), and the diffusion coefficients measured in this layer using 3D FES [28] (b).

Summary

The possibility to measure diffusion coefficients in poly-crystalline thin films using finite element simulation is discussed. It is shown that 2D FES allows to measure simultaneously the lattice and the GB diffusion coefficients from a single 1D experimental composition profile. The possibility to measure lattice diffusion in the grains of poly-crystalline layers during the diffusion kinetic regime *B* offers the opportunity to measure lattice diffusion at lower temperature than that usually used for experiments performed in mono-crystals, as well as to study lattice diffusion in nanometric phases in the case of nano-crystalline samples. 2D FES allows also to take into account GB segregation during diffusion experiments, and to extract effective GB diffusion coefficients in the case of experiments with moving GBs. 3D FES can also be performed. One of their applications is the ability to measure TJ diffusion coefficients and lattice diffusion in grains, if the GB diffusion coefficient is known.

Acknowledgements

The authors would like to thank Philippe Maugis (Aix-Marseille University, formerly at ARCELOR) and Lorenzo Ciampolini (STMicroelectronics) for interesting discussions.

References

- [1] H. Mehrer: *Diffusion in Solids* (Springer-Verlag, Berlin Heidelberg, 2007).
- [2] P. Pichler: *Intrinsic Point Defects, Impurities, and their Diffusion in Silicon* (Springer-Verlag/Wien New York, Austria, 2004).
- [3] <http://www.itrs.net>.
- [4] P. Pichler, A. Burenkov, J. Lorenz, C. Kampen, and L. Frey: *Thin Solid Films* Vol. 518 (2010), p. 2478.
- [5] J.A. Sethian and J. Wilkening: *J. Comput. Phys.* Vol. 193 (2003), p. 275.
- [6] H.N. Ch'ng and J. Pan: *J. Comput. Phys.* Vol. 196 (2004), p. 724.
- [7] H.M. Mourad and K. Garikipati: *Comput. Methods Appl. Mech. Engrg.* Vol. 196 (2006), p. 595.

- [8] Y. Wei, F. Bower and H. Gao: *J. Mech. Phys. Solids* Vol. 56 (2008), p. 1460.
- [9] W. Preis and W. Sitte: *Solid State Ionics* Vol. 179 (2008), p. 765.
- [10] M. Pernach and M. Pietrzyk: *Comput. Mater. Sci.* Vol. 44 (2008), p. 783.
- [11] D. Gryaznov, J. Fleig, and J. Maier: *Sol. State Sci.* Vol 10 (2008), p. 754.
- [12] F. Fournier, D. Chabert, F. Tancret, F. Christien, R. Le Gall, and J.-F. Castagné : *J. Mater. Sci.* Vol. 42 (2007), p. 9765.
- [13] A. Portavoce, R. Simola, D. Mangelinck, J. Bernardini, and P. Fornara: *Diff. Def. Data* Vol. 264 (2007), p. 33.
- [14] L.G. Harrison: *Trans. Faraday Soc.* Vol. 57 (1961), p. 1191.
- [15] J.C. Fisher: *J. Appl. Phys.* Vol. 22 (1951), p. 74.
- [16] A. Fick: *Phil. Mag. S.* Vol. 10 (1855), p. 30.
- [17] A. Portavoce, N. Rodriguez, R. Daineche, C. Grosjean, and C. Girardeaux: *Mater. Lett.* Vol. 63 (2009), p. 676.
- [18] I. Blum, A. Portavoce, D. Mangelinck, R. Daineche, K. Hoummada, J. L. Lábár, V. Carron, and C. Perrin: *J. Appl. Phys.* Vol. 104 (2008), p. 114312.
- [19] I. Blum, A. Portavoce, D. Mangelinck, R. Daineche, K. Hoummada, J.L. Lábár, V. Carron, and J. Bernardini: *Microel. Eng.* Vol. 87 (2010), p. 263.
- [20] C. E. Allen, D. L. Beke, H. Bracht, C. M. Bruff, M. B. Dutt, G. Erdélyi, P. Gas, F. M. d'Heurle, G. E. Murch, E. G. Seebauer, B. L. Sharma, and N. A. Stolwijk, in: *Diffusion in Semiconductors and Non-Metallic Solids*, Landolt-Börnstein-Numerical Data and Functional Relationships in Science and Technology, edited by D. Beke (Springer-Verlag, Berlin, 1998), Vol. 33.
- [21] H. Bakker, H. P. Bonzel, C. M. Bruff, M. A. Dayananda, W. Gust, J. Horváth, I. Kaur, G. V. Kidson, A. D. Le Claire, H. Mehrer, G. E. Murch, G. Neumann, N. Stolica, and N. A. Stolwijk, in: *Diffusion in Solid Metals and Alloys*, Landolt-Börnstein-Numerical Data and Functional Relationships in Science and Technology, edited by H. Mehrer (Springer-Verlag, Berlin, 1990), Vol. 26.
- [22] A. Portavoce, G. Chai, L. Chow, and J. Bernardini: *J. Appl. Phys.* Vol. 104 (2008), p. 104910.
- [23] P. Dorner, W. Gust, B. Predel, U. Roll, A. Lodding, and H. Odelius: *Philos. Mag. A* Vol. 49 (1984), p. 557.
- [24] G. Hettich, H. Mehrer, and K. Maier: *Inst. Phys. Conf. Ser.* Vol. 46 (1979), p. 500.
- [25] N.R. Zangenberg, J. Lundsgaard Hansen, J. Fage-Pedersen, and A. Nylandsted Larsen: *Phys. Rev. Lett.* Vol. 87 (2001), p. 125901.
- [26] F. Nemouchi, D. Mangelinck, C. Bergman, P. Gas, and U. Smith: *Appl. Phys. Lett.* Vol. 86 (2005), p. 041903.
- [27] A. Portavoce, D. Mangelinck, R. Simola, R. Daineche, and J. Bernardini: *Defect and Diffusion Forum* Vols. 289-292 (2009), p. 329.
- [28] A. Portavoce, L. Chow, and J. Bernardini: *Appl. Phys. Lett.* Vol. 96 (2010), p. 214102.
- [29] J.-C. Ciccariello, S. Poize, and P. Gas: *J. Appl. Phys.* Vol. 67 (1990), p. 3315.

Grain Boundary Diffusion, Stresses and Segregation

doi:10.4028/www.scientific.net/DDF.309-310

Numerical Simulation Support for Diffusion Coefficient Measurements in Polycrystalline Thin Films

doi:10.4028/www.scientific.net/DDF.309-310.63